The effects of inescapable stress on leukocyte subpopulations in male rats previously treated with *Mycobacterium vaccae* NCTC 11659

By

Andrew Kyo Lee

Department of Psychology and Neuroscience

Department of Molecular, Cellular, and Developmental Biology

Defense Date: Friday, April 2 2021

Thesis Advisor:

Dr. Christopher A. Lowry, Department of Integrative Physiology and Center for Neuroscience

Defense Committee:

Dr. Alison Vigers, Department of Psychology and Neuroscience, Honors Council Representative

Dr. Corrie Detweiler, Department of Molecular, Cellular, and Developmental Biology, Committee Member

Dr. Heidi Day, Department of Psychology and Neuroscience, Committee Member

Table of Contents

Abstract:

Inappropriate inflammation has been linked to stress-related psychiatric disorders such as depression, anxiety, and posttraumatic stress disorder (PTSD). Inflammation is associated with increased proinflammatory cytokines, such as interleukin 1 beta (IL-1β), interleukin 23 (IL-23), and interleukin 6 (IL-6). Increasing evidence suggests that the microbiome, particularly a category of microorganisms referred to as "old friends" is an important determinant of the balance between regulatory and effector T cell populations (i.e., immunoregulation). However, how these "old friends" are able to exert their immunoregulatory effects is not fully understood. *Mycobacterium vaccae* (*M. vaccae*), a saphrophytic mycobacterium, has been shown to have a protective effect on depressive- and anxiety-like behaviors in several animal models of stress. For example, *M. vaccae* has been shown to have stress resilience effects in male rats after exposure to inescapable tail shock stress (IS), as assessed by the juvenile social exploration (JSE) test, in a model of learned helplessness, but the mechanism of how it achieves these effects is not fully understood. Previous research using stress models such as repeated social defeat (RSD) have shown that anxiety- and depressive-like behaviors are associated with an increase of circulating Ly6C^{hi} inflammatory monocytes in mice. One hypothesis is that *M. vaccae* may be exerting its effects in part through its interaction with these inflammatory monocytes. This experiment is a pilot study that characterized leukocyte subpopulations after IS in rats using a previously established nine-color immunophenotyping panel that identified neutrophils, inflammatory and anti-inflammatory monocytes, natural killer (NK) cells, B cells, and CD4+ and CD8+ T cells. Compared to home cage (HC) controls, IS increased neutrophils but decreased lymphocytes in the peripheral blood 6 hours after IS. Additionally, IS increased the relative proportion of inflammatory monocytes, suggesting that the stress-induced effects of IS may be due in part to the increase of the relative percentage of inflammatory monocytes. This study supports the hypothesis that inflammatory monocytes are involved in the pathogenesis of stress-induced anxiety-like defensive behavioral responses and corroborates with previous lines of research characterizing leukocyte subpopulations after stress.

Abbreviations:

ACK, ammonium-chloride-potassium

APC, allophycocyanin

APC-Cy7, allophycocyanin-cyanine7

BBS, borate-buffered saline

BM, bone marrow

BUV396, bright ultra-violet 396

BUV496, bright ultra-violet 496

CCL2, c-c chemokine ligand type 2

CCR2, c-c chemokine receptor type 2

CD, cluster of differentiation

EDTA, ethylenediaminetetraacetic acid

FBS, fetal bovine serum

Fc, fragment crystallizable

FITC, fluorescein isothiocyanate

FMO, fluorescence minus one

FSC, forward-scatter

GC, glucocorticoid

HC, home cage

HPA, hypothalamic-pituitary-adrenal

IACUC, Institutional Animal Care and Use Committee

IL, interleukin

IS, inescapable tail shock stress

ITI, inter-trial interval

JSE, juvenile social exploration

LLT, lavender top tubes

LPS, lipopolysaccharide

Ly6C, lymphocyte antigen 6 complex, locus C1

MdFI, median fluorescence intensities

NE, norepinephrine

NK, natural killer

NCTC, National Collection of Type Cultures

NF-κB, nuclear factor kappa-light-chain-enhancer of activated B cells

PBS, phosphate buffered saline

PE, phycoerythrin

PerCP-Cy5.5, peridinin chlorophyll protein-cyanine5.5

PTSD, posttraumatic stress disorder

RSD, repeated social defeat

s.c., subcutaneous

SD, Sprague Dawley

SSC, side-scatter

Treg, regulatory T cells

Veh, vehicle

ZT, zeitgeber

1. Introduction

Stress-related psychiatric disorders, such as depression, anxiety, and posttraumatic stress disorder (PTSD), places a significant amount of distress and financial burden within the U.S. and across countries worldwide (Judd et al., 1996; Kessler & Greenberg, 2002; Kessler, 2000). Previous research has shown that inflammation may play a significant role in stress-related psychiatric disorders (Dantzer et al., 2008; Davis et al., 2017; Xu et al., 2020). Multiple convergent lines of evidence in humans and animal models suggest that inappropriate peripheral inflammation is indeed a risk factor for the development of stress-related psychiatric disorders (Miller & Raison, 2016; Reader et al., 2015). The microbiome has gained a considerable amount of attention for its ability to regulate stress-related behavioral responses by mediating inflammatory and metabolic signaling, which provides an exciting and novel opportunity to investigate new prevention and treatment strategies for stress-related psychiatric and neurological disorders (Kelly et al., 2017; Kipnis, 2018; Lowry et al., 2016).

Evidence suggests that inappropriate inflammation may be attributed to decreased numbers or function of regulatory T cells (Treg) secondary to decreased exposure to the microorganisms that humans once co-evolved with such as saprophytic mycobacteria, helminths, and lactobacilli (Rook et al., 2004). Exposure to these "old friends" may help promote anti-inflammatory signaling, thereby increasing stress resilience (Lowry et al., 2016; Rook et al., 2014). *Mycobacterium vaccae* (*M. vaccae* NCTC 11659), a type of saprophytic mycobacteria, has been shown to promote stress-resilience and decrease anxiety-like and depressive-like behaviors in both mouse and rat behavioral models (Amoroso et al., 2020; Bowers et al., 2020; Fonken et al., 2018; Foxx et al., 2020; Loupy et al., 2019; Loupy et al., 2021). Previous research has shown that *M. vaccae* activates immune-responsive mesolimbocortical brain serotonergic systems in the dorsal raphe nucleus (Lowry et al., 2007). The mechanisms through which *M. vaccae* NCTC 11659 achieves these effects, however, are not fully understood.

Prior investigation suggests that Tregs may play a role in stress resilience effects of *M. vaccae* NCTC 11659 by increasing immunoregulation since *M. vaccae* NCTC 11659 has been shown to increase Tregs in the

spleen using a mouse model of allergic pulmonary inflammation (Zuany-Amorim et al., 2002). Additionally, suppressing Tregs in mice using anti-interleukin-2 receptor alpha (anti-CD25) antibody was shown to attenuate the anxiolytic effects on stress-induced behavior produced by *M. vaccae* NCTC 11659 (Reber et al., 2016). On the other hand, chronic psychological stress in humans has been shown to increase proinflammatory-related gene expression in the nuclear factor kappa-light-chain-enhancer of activated B cells (NF-κB) transcriptional pathway in peripheral monocytes (Miller & Raison, 2016; Miller et al., 2008). An alternative hypothesis is that *M. vaccae* NCTC 11659 prevents the stress-induced mobilization of inflammatory monocytes from the bone marrow, activation of these cells, or trafficking of inflammatory monocytes to the central nervous system.

Hematopoiesis and the differentiation of monocytes occur within the bone marrow (BM), which is innervated by descending sympathetic nerve fibers that release norepinephrine (NE) (Weber et al., 2017). Repeated social defeat (RSD), where a naïve mouse is exposed to a large aggressor mouse, can cause a release of NE in the bone marrow, which increases the myelopoietic output of primed glucocorticoid (GC) insensitive inflammatory monocytes (Powell et al., 2013). Furthermore, these inflammatory monocytes, identified as $CD14^{++}CD16^{+}$ intermediate inflammatory or $CD14^{+}CD16^{++}$ nonclassical monocytes in humans (Hasselmann et al., 2018; Yang et al., 2014); $Ly6C^{hi}$ monocytes in mice, and $CD43^{lo}$ monocytes in rats (Barnett-Vanes et al., 2016), were shown to be recruited to the brain following psychosocial stress, and are believed to contribute to stress-induced behaviors such as stress-induced increases in anxiety-like defensive behavioral responses (Miller & Raison, 2016; Powell et al., 2013; Reader et al., 2015; Wohleb, McKim, Sheridan, et al., 2014). It is important to note however that not all rodent stress models are able to elicit the same myelopoietic response, as certain stressors can produce an immunosuppressive response due to increases in resting GC levels, as seen in chronic restraint stress models (Weber et al., 2017). One factor in the RSD model that may contribute to the priming of GC-insensitive monocytes in the BM is the wounding associated with the bite that comes from the aggressor (Weber et al., 2017). Wounding can increase bacteria and lipopolysaccharide (LPS) in the blood, which activates toll-like receptor 4 (TLR4) on circulating monocytes, driving them toward an inflammatory phenotype (Foertsch et al., 2017).

M. vaccae NCTC 11659 prevents stress-induced reductions in exploratory behavior in the juvenile social exploration (JSE) paradigm after exposure to inescapable tail shock stress (IS) (Frank et al., 2018; Loupy et al., 2021). Although stress-induced microglial priming was observed after IS (Frank et al., 2018), differences in monocyte populations after IS have not yet been characterized. Furthermore, there were no differences seen in the relative abundance of Tregs between control and *M. vaccae* groups in a subsequent study (Loupy et al., 2021), which indicates a need for a more comprehensive analysis of what is occurring in the peripheral blood of rats in the IS paradigm. Given the fact that IS increases lipopolysaccharide (LPS) in circulation (Maslanik et al., 2012), which is known to shift circulating monocytes toward an inflammatory phenotype (Miller & Raison, 2016), it is likely that IS will induce an increase in inflammatory monocytes similar to RSD. This study is an explorative survey of the effects of IS on leukocyte subpopulations in the peripheral blood in both *M. vaccae* NCTC 11659 immunized rats and borate-buffered saline- (BBS-) treated control rats using a multicolor flow cytometry panel that has been validated to immunophenotype neutrophils, inflammatory and anti-inflammatory monocytes, natural killer (NK) cells, B cells, CD4+ and CD8+ T cells (Barnett-Vanes et al., 2016). Characterizing the changes in leukocyte subpopulations after IS may help our understanding of how *M. vaccae* NCTC 11659 achieves its stress-resilience effects, such as those seen in the JSE paradigm after exposure to IS.

2. Methods

2.1. Animals

For an experimental timeline, please see **Fig. 1**. Adult male Sprague Dawley® (SD) rats (Strain code 400, Crl:SD; Charles River, Wilmington, MA, USA) weighing 250-265 g upon arrival, were pair-housed in standard Static Allentown micro isolator filter-topped polysulfone rat cages; cage model # PC10198HT cage top: # MBT1019HT; (25.9 cm x 47.6 cm x 20.9 cm) (Static Allentown, Allentown, NJ, USA). The cages contained approximately 2.5 cm-deep layer of bedding (Cat. No. 7090; Teklad Sani-Chips; Envigo, Huntingdon, United Kingdom). All rats were kept under standard laboratory conditions (12-h light/dark cycle, lights on at 0700 h, 22 °C) and had free access to water and a standard rat diet (Harlan Teklad 2918 Envigo,

Huntingdon, United Kingdom). Cages were changed once per week. The study was consistent with the National Institutes of Health's *Guide for the Care and Use of Laboratory Animals, Eighth Edition* (The National Academies Press, 2011), and all procedures within this study was approved by the Institutional Animal Care and Use Committee (IACUC) at the University of Colorado Boulder. All possible efforts were made to minimize the number of animals used and their suffering. In addition, all studies followed *The ARRIVE guidelines 2.0: Updated guidelines for reporting animal research* (Percie du Sert et al., 2020).

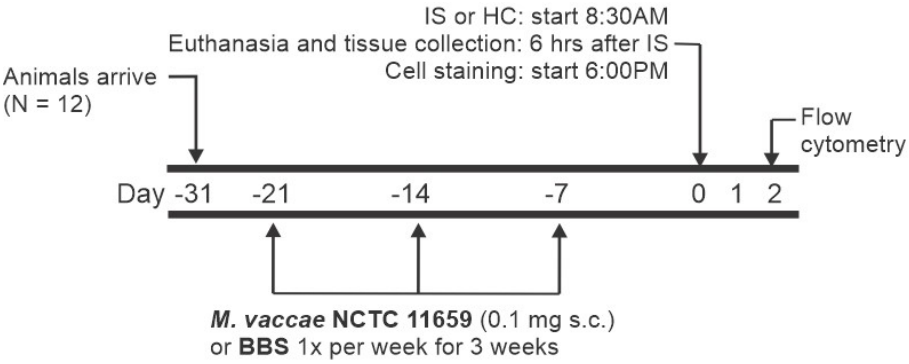

Fig. 1. Schematic for representing the experimental timeline for *M. vaccae* NCTC 11659 or vehicle (borate-buffered saline [BBS] treatment in relation to exposure to inescapable shock (IS), euthanasia, tissue collection, and flow cytometry. $N = 12$ adult male Sprague Dawley® (SD) rats received three immunizations consisting of subcutaneous (s.c) injections of either *M. vaccae* NCTC 11659 or vehicle control (BBS) on days –21, –14, and –7 and were subsequently exposed to inescapable tail shock stress (IS) or home cage (HC) control conditions on day 0. Abbreviations: BBS, borate-buffered saline; IS, inescapable tail shock stress; SD, Sprague Dawley®; s.c., subcutaneous; HC, homecage.

2.2. M. vaccae and vehicle immunization

Experimental rats received repeated subcutaneous injections of either vehicle (Veh) or 0.1 mg of a whole-cell, heat-killed preparation of *M. vaccae* NCTC 11659 (10 mg/ml suspension diluted to 1 mg/ml in sterile filtered BBS, batch ENG 1, Bio Elpida, Lyon, France) with injection sites between the scapulae on days –21, –14, and –7. Each immunization was performed using 21-gauge needles (Cat. no. 315165, BD Biosciences,

San Jose, CA, USA) between zeitgeber (ZT) 2–4 to ensure the transmission of larger particulates in the whole-cell suspension. Dilutions of *M. vaccae* NCTC 11659 material from stock suspensions provided by Bio Elpida were prepared immediately prior to injections in a single siliconized 1.5 ml microcentrifuge tube (Cat. no. 416556, Bio Plas, San Rafael, CA, USA). The dose used (0.1 mg; estimated to be 1×10^8 bacteria) was 1/10 of the dose used in human studies (1 mg) (O'Brien et al., 2004), and was identical to the dose used in previous studies in rats (Fonken et al., 2018; Fox et al., 2017; Frank et al., 2018; Hassell et al., 2019; Loupy et al., 2019; Loupy et al., 2021).

2.3. Inescapable tail shock (IS)

Procedures for IS were performed as previously described (Frank et al., 2018). Briefly, rats were placed in Plexiglas® tubes (23.4 cm in length × 7 cm in diameter) and were then exposed to 100 1.6 mA, 5-s tail shocks with a variable inter-trial interval (ITI) ranging from 30 to 90 s (average ITI = 60 s). All IS treatments occurred between 8:30 AM and 11:00 AM. IS animals were returned to their home cages immediately after termination of the IS testing. Home cage control (HC) animals remained undisturbed in their home cages.

2.4. Tissue collection

Rats from both groups were euthanized 6 hours after IS by lethal intraperitoneal (i.p.) pentobarbital injection (Fatal Plus®, Vortech Pharmaceuticals Ltd., Dearborn, MI, USA; 200 mg/kg.). The timeframe between IS exposure and euthanasia was chosen based on a previous study showing increased inflammatory monocytes in the blood 0.5 days after RSD (Wohleb 2014). Additionally, experimentation and euthanasia of all rats occurred within their 12 h inactive period (7:00 AM-7:00 PM) to avoid confounding variables produced by the circadian rhythmicity of corticosterone, which has been previously shown to affect the distribution of peripheral blood leukocyte subpopulations (Dhabhar et al., 1994).

Following euthanasia and opening the thoracic cavity, whole blood was collected via cardiac puncture, which yielded the largest quantity of blood with the least amount of contamination in the quickest amount of

time. Around 5-8 mL of blood per animal was collected by cardiac puncture. A 25 gauge needle and a 10 mL Luer Lock syringe was used to draw the blood from the left ventricle of the heart and dispensed into vacutainer lavender top tubes (LLT) pre-coated with ethylenediaminetetraacetic acid (EDTA) as a decoagulant. Final sample sizes for flow cytometry were BBS/HC, $n = 4$; BBS/IS, $n = 4$; *M. vaccae* NCTC/HC, $n = 2$; *M. vaccae* NCTC/IS, $n = 2$.

2.5. Preparing single cell suspensions using whole blood

The LTTs containing whole blood samples were centrifuged at 2,000 x g at 4 °C. After centrifugation, three visible layers in the blood sample were observed. The plasma in the clear supernatant on top was aspirated and placed into 1.5 mL microcentrifuge tubes and placed in liquid nitrogen prior to storing in a –80 °C freezer until further downstream analysis. Leukocytes were isolated by aspirating the white-colored buffy coat (**Fig. 2**) into 15 mL Falcon conical centrifuge tubes.

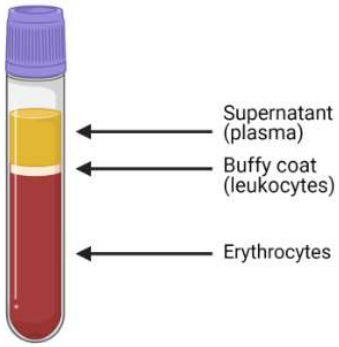

Fig. 2. Centrifuged blood that has separated into three distinct layers, created with BioRender.com.

Erythrocyte lysis was performed in the leukocyte preparation by adding 10 mL of 1X ammonium-chloride-potassium (ACK) buffer (0.155 M NH_4Cl, 0.01 M $KHCO_3$, 0.1 mM EDTA) into the Falcon tubes. Samples were then incubated at room temperature for 5 minutes and were centrifuged at 300 x g at room temperature for 5 minutes. The supernatant was removed and the cells were resuspended in phosphate buffered

saline (PBS) and centrifuged at 300 x g at 4 °C for 5 minutes. Once again, the supernatant was removed and cells were resuspended in PBS. Viability and concentration of cells in each suspension was confirmed by staining cells with a 1:1 dilution of trypan blue. Stained cells were observed and counted using a hemocytometer under a microscope at 1000X magnification. Live leukocytes were identified by the absence of trypan blue stain, morphology, and size. Suspensions were diluted to obtain a concentration of 2 x 10^6 cells/mL. A pool of cells for single stain and fluorescence minus one (FMO) controls was collected by transferring 500 uL of each previously prepared single cell suspension into another 15 mL Falcon tube.

2.6. Flow cytometry panel and cell staining

A nine-color flow panel (**Table 1**) was designed based on the markers and the gating strategy used in a previous established rat immunophenotyping panel (Barnett-Vanes et al., 2016). Prior to staining, cells were transferred into a 96-V bottom well plate and kept on top of wet ice. Cells were first stained with Live/Dead Fixable Yellow dye (Invitrogen™) in PBS and washed. To prevent fragment crystallizable (Fc)-mediated non-specific binding, cells were then blocked with 50 uL anti-CD32 antibody at 2X the concentration in flow buffer (PBS, 2% fetal bovine serum (FBS), 5 mM EDTA, and 0.1% sodium azide). Cells were then stained with 50 uL of the remaining antibodies with a master mix containing antibodies in 2X concentration in flow buffer, resulting in a final concentration of 1X for both the Fc-block and antibodies in a total volume of 100 uL of flow buffer. Cells were then washed with flow buffer and fixed using a stabilizing fixative (Cat. No: 338036, BD™). To prevent antibody degradation from the fixative, samples were washed and resuspended in flow buffer prior to storage. Samples were kept at 4 °C and wrapped in foil to prevent fluorochrome photobleaching and were analyzed 24 hours later.

Table 1. Flow cytometry panel of monoclonal antibodies used for rat whole blood immunophenotyping

Antibody	Fluorochrome	Clone	Catalogue #, Supplier	Dilution	Laser	Filter
CD32	----------	D34-485	550270, BD Pharmingen	1 : 200	N/A	N/A
Live-Dead	Live/Dead yellow	---------	L34967, Thermofisher	1 : 200	Violet-405	525/50
CD45	APC-Cy7	OX-1	561586, BD Pharmingen	1 : 100	Red-633	780/60
CD3	PE	G4.18	554833, BD Pharmingen	1 : 100	Blue-488	575/26
CD4	APC	OX-35	550057, BD Pharmingen	1 : 200	Red-633	730/35
CD8	BUV496	OX-8	741106, BD Horizon	1 : 200	UV-355	740/35
CD161	BUV395	C10/78	744055, BD Optibuild	1 : 200	UV-355	379/28
CD45R	PE-Cyanine7	His24	25-0460-82, eBioscience	2 : 200	Red-633	730/45
CD43	PerCP-Cy5.5	W3/13	202818, Biolegend	1 : 200	Red-633	710/50
His48	FITC	His48	554907, BD Pharmingen	1 : 200	Blue-488	525/50

2.7 Voltage calibration

Data were acquired using BD FACSDiva Software (Diva) (version 9.0, BD Biosciences) on a BD LSR II Flow Cytometer (BD Biosciences), located in the Division of Allergy, Asthma and Clinical Immunology Flow Core at the University of Colorado Anschutz Medical Campus (Aurora, CO, USA). In order to achieve an optimal resolution, voltages were calibrated visually using the Cell Analyzer in Diva using aliquots of unstained and single stained samples. An unstained sample was first used to obtain a general assessment of the amount of auto-fluorescence of cells and to optimally establish voltages for forward-scatter (FSC) and side-scatter (SSC). Next, an aliquot of each single stain control was used to set voltages. Optimal voltages were visually confirmed by ensuring that negative and positive populations were distinct and within scale with minimal presence of background noise.

2.8. Compensation using Diva

Acquisition and initial calculation of compensation controls was automatically performed through Diva by running single stained samples. All antibodies except for Live/Dead yellow were set using single-stained compensation bead controls (UltraComp eBeads™, Cat. No: 01-222-41, Invitrogen™, Carlsbad, CA, USA) that were prepared according to the manufacturer's instructions. Since amine reactive dyes do not bind to UltraComp eBeads, the compensation sample for Live/Dead yellow was created by staining a mixture 50 uL of pool cells and 50 uL of pool cells that were killed by treatment with 70% isopropyl alcohol. After compensation was set, single-stained samples were ran through the flow cytometer for analysis, followed by FMO controls and experimental samples. Raw data were then imported to FlowJo Software (version 10.7.1, FlowJo, LLC., Ashland, OR, USA) for further analysis.

2.9. Compensation check using FlowJo

The compensation matrix acquired using Diva was checked in FlowJo by individually plotting all nine fluorophore compensation parameters against each other, producing 72 plots (9 x 8). Compensation was initially checked by eye by adjusting the compensation matrix so that the median fluorescence intensities (MdFI) of the negative and positive populations were as equal as possible in all plots. After a visual check, negative and positive populations were gated and compensation was manually adjusted by calculating the MdFI of the gated positive and negative populations using FlowJo. The compensation matrix was adjusted so that the MdFI of positive and negative populations were as equal as possible, deviating no more than +/– 20 (**Fig. 3**).

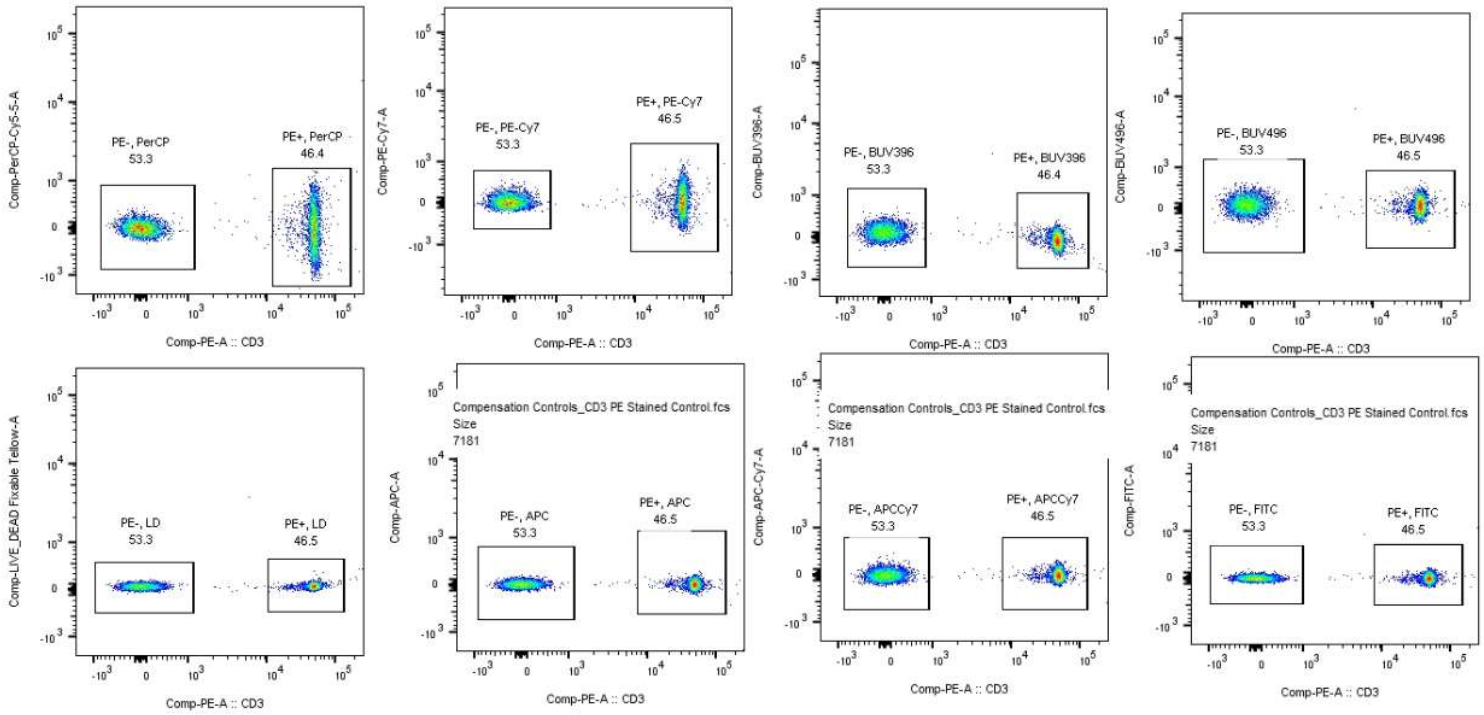

Fig. 3. Example of manual compensation check of CD3 with positive and negative populations gated, adjusted so that the median fluorescence intensity (MdFI) difference between positive and negative gates were as equal as possible, deviating by no more than 20. Abbreviations: MdFI, median fluorescence intensity; Comp-PE-A CD3, compensated phycoerythrin; Comp-PerCP-Cy5.5-A, compensated peridinin chlorophyll protein-cyanine5.5; Comp-BUV396-A, compensated bright ultra-violet 396; Comp-BUV496-A, compensated bright ultra-violet 496; Comp-Live_Dead Fixable Tellow-A, compensated live/dead fixable yellow; Comp-APC-A, compensated allophycocyanin; Comp-APC-Cy7-A, compensated allophycocyanin cyanine7; Comp-FITC-A, compensated fluorescein isothiocyanate.

2.10. Gating strategy

The gating strategy (**Fig. 4**) first excluded any cells that were not singlets by using FSC (**Fig. 4A**), followed by an additional doublet exclusion using SSC (**Fig. 4B**). Debris was then excluded by applying a schmutz gate using FSC and SSC (**Fig. 4C**), and dead cells identified and excluded based on Live/Dead yellow staining (**Fig. 4D**). Cells that were positive for CD45 were gated as "leukocytes" (**Fig. 4E**). Within the leukocyte population, T cells were gated based on cells positive for CD3 (**Fig. 4F**). A quadrant gate was then set on cells positive for CD3 using CD4 and CD8 as parameters and $CD3^{+}CD4^{+}$ and $CD3^{+}$ $CD8^{+}$ T cells were identified (**Fig. 4G**). Cells that were CD3– were then gated using His48 and CD161 as parameters. Cells that were $CD161^{+}His48^{-}$ were gated as NK cells (**Fig. 4H**). Cells that were not $CD161^{+}His48^{-}$ were then gated using CD161 and CD45R as parameters and CD45R+ cells were gated as B cells (**Fig. 4I**). Cells that were $CD45R^{-}$ were then gated based on CD43 expression. Neutrophils were gated based on their granularity using SSC (**Fig. 4J**). The remaining cells were then gated using His48 and CD43 as parameters. Non-inflammatory monocytes were identified based on $CD43^{Hi}His48^{Low\text{-}Intermediate}$ expression and inflammatory monocytes were gated based on $CD43^{Lo}His48^{Hi}$ expression (**Fig. 4K**). Gates were refined and checked using an unstained control for autofluorescence and all FMO controls (**Fig. 5**).

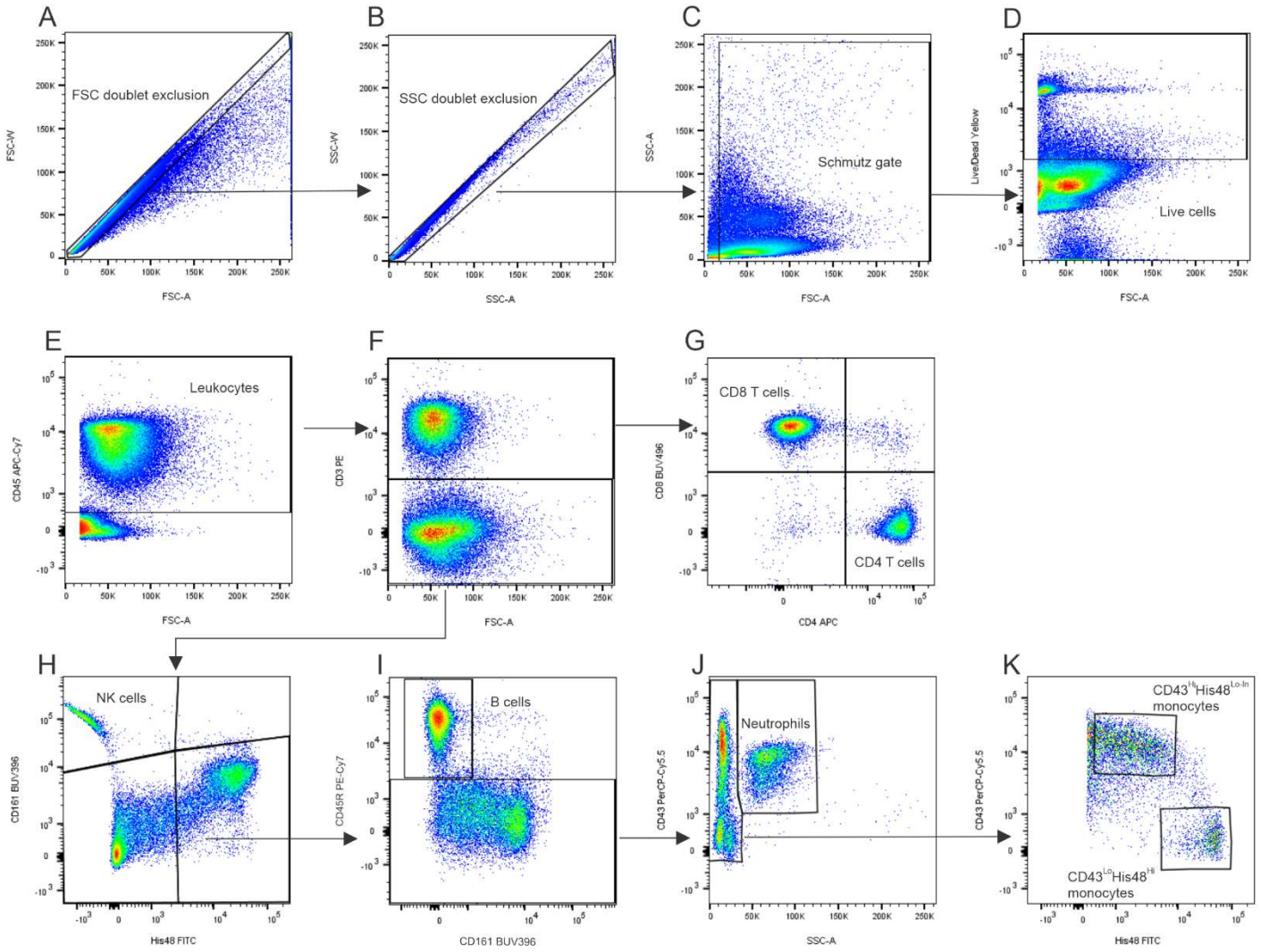

Fig. 4. Flow cytometry gating strategy to identify major leukocyte subpopulations in rat whole blood. Singlets were isolated using forward scatter width (FSC-W) (**A**) and side scatter width (SSC-W) (**B**), debris was removed (**C**) and dead cells were excluded (**D**). Leukocytes were then identified (**E**) and T cells were gated (**F**), further distinguished into $CD8^+$ and $CD4^+$ T cells (**G**). Natural killer (NK) cells were gated (**H**) followed by B cells (**I**). Neutrophils were gated based on SSC properties of granularity (**J**) and finally non-inflammatory and proinflammatory monocytes were gated based on differential expression of CD43 and His48 (**K**).

Abbreviations: FSC-W, forward scatter width; FSC-A, forward scatter area; SSC-W, side scatter width; SSC-A, side scatter area; NK, natural killer; PE, phycoerythrin; PerCP-Cy5.5, peridinin chlorophyll protein-cyanine5.5; BUV396, bright ultra-violet 396; BUV496, bright ultra-violet 496; APC, allophycocyanin; APC-Cy7, allophycocyanin-cyanine7; FITC, fluorescein isothiocyanate.

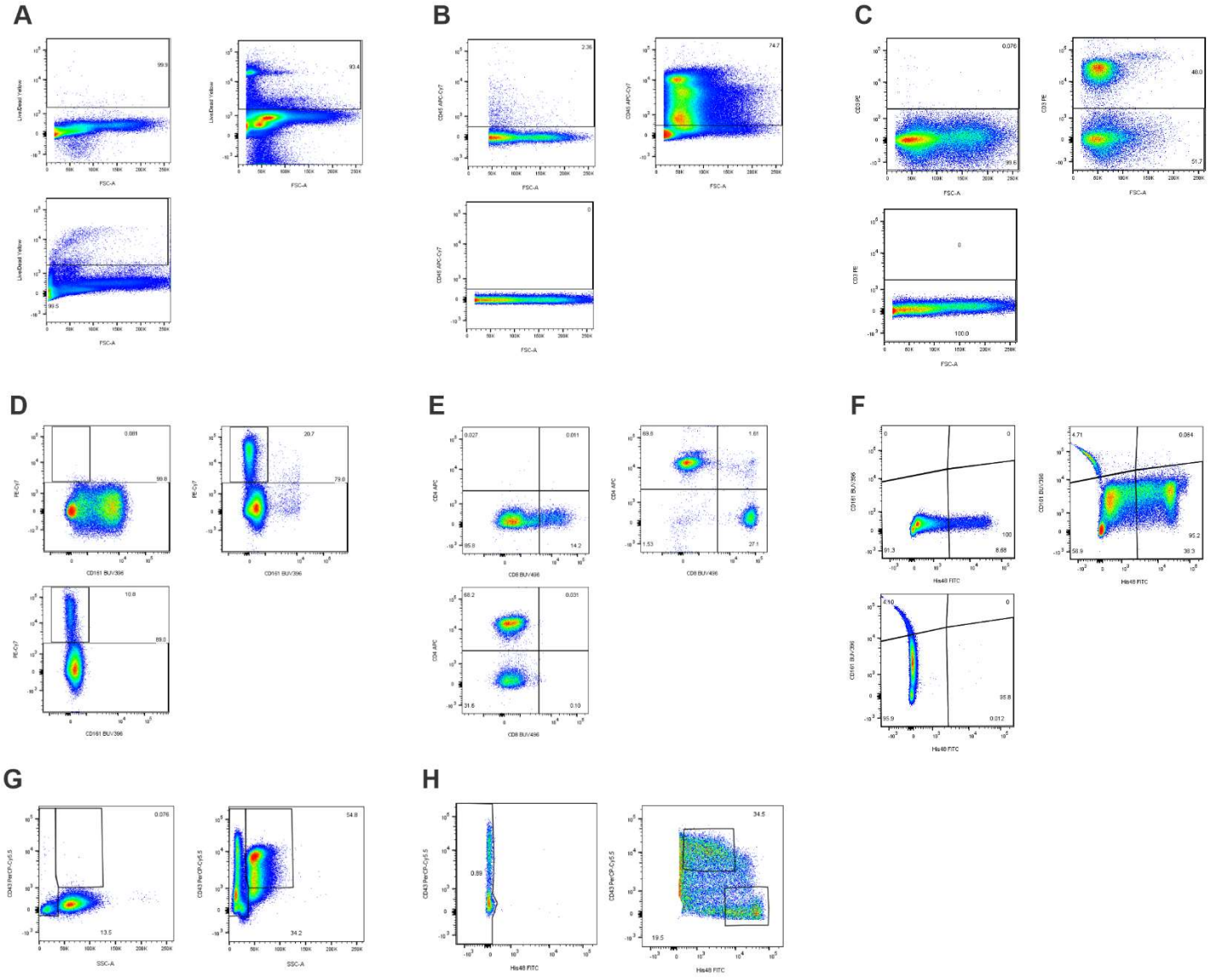

Fig. 5. Fluorescence minus one (FMO) controls used to refine gates for Live/Dead yellow (**A**), CD45 (**B**), CD3 (**C**), CD161 (**D**), CD4 and CD8 (**E**), His48 (**F**), CD43 and His48 (**G**) CD43 and (**H**) His48. Abbreviations: FMO, fluorescence minus one.

2.11. Quantification of blood immune cell subpopulations

Immune cell populations were quantified using FlowJo by calculating the relative percentage of the subpopulation out of the total number of leukocytes. Comparisons were made using the relative percentage out

of all leukocytes to normalize values since the total number of cells and the total number of leukocytes varied among samples. The relative percentage out of all leukocytes was calculated for CD3+ T cells, CD4+ T cells, CD8+ T cells, B cells, NK cells, neutrophils, and monocytes. Monocytes were then further quantified by calculating the relative percentage of each monocyte subtype out of the total number of monocytes.

2.12. Statistical analysis

M. vaccae NCTC 11659/HC and *M. vaccae* NCTC 11659/IS treatment groups were excluded from statistical analysis and were only qualitatively analyzed since there were not enough subjects per treatment group ($n = 2$). The relative percentage of each subpopulation out of all leukocytes in BBS/HC and BBS/IS groups ($n = 4$) were first tested for normality with the Shapiro-Wilk test using R Statistical Programing (version 4.0.4). Differences in group variances were then tested using Levene's Test of Equality in Microsoft Excel. Because homoscedasticity was established for all subpopulations except for neutrophils, the Welch's *t*-test was used to analyze neutrophils while Student's *t*-tests were used for all other subpopulations. In all bar graphs, bars represent the mean + standard deviation of the mean.

3. Results

3.1. Effect of IS on the distribution of leukocyte subtypes

Fig 6A and **Table 2** illustrate IS-induced changes in the percentages of peripheral blood leukocyte subpopulations. When comparing BBS/HC animals to BBS/IS animals, there was a significant reduction of the relative abundances of T cells [$t(6) = 6.79$, $p < 0.001$], monocytes [$t(6) = 4.34$, $p < 0.01$], and NK cells [$t(6) = 4.30$, $p < 0.01$], along with a significant increase of neutrophils [$t(3) = -6.54$, $p < 0.01$]. There was no statistical difference in the relative abundance of B cells between both groups [$t(6) = 0.77$, $p = 0.47$]. The same trend was qualitatively observed when comparing *M. vaccae*/HC animals to *M. vaccae*/IS animals.

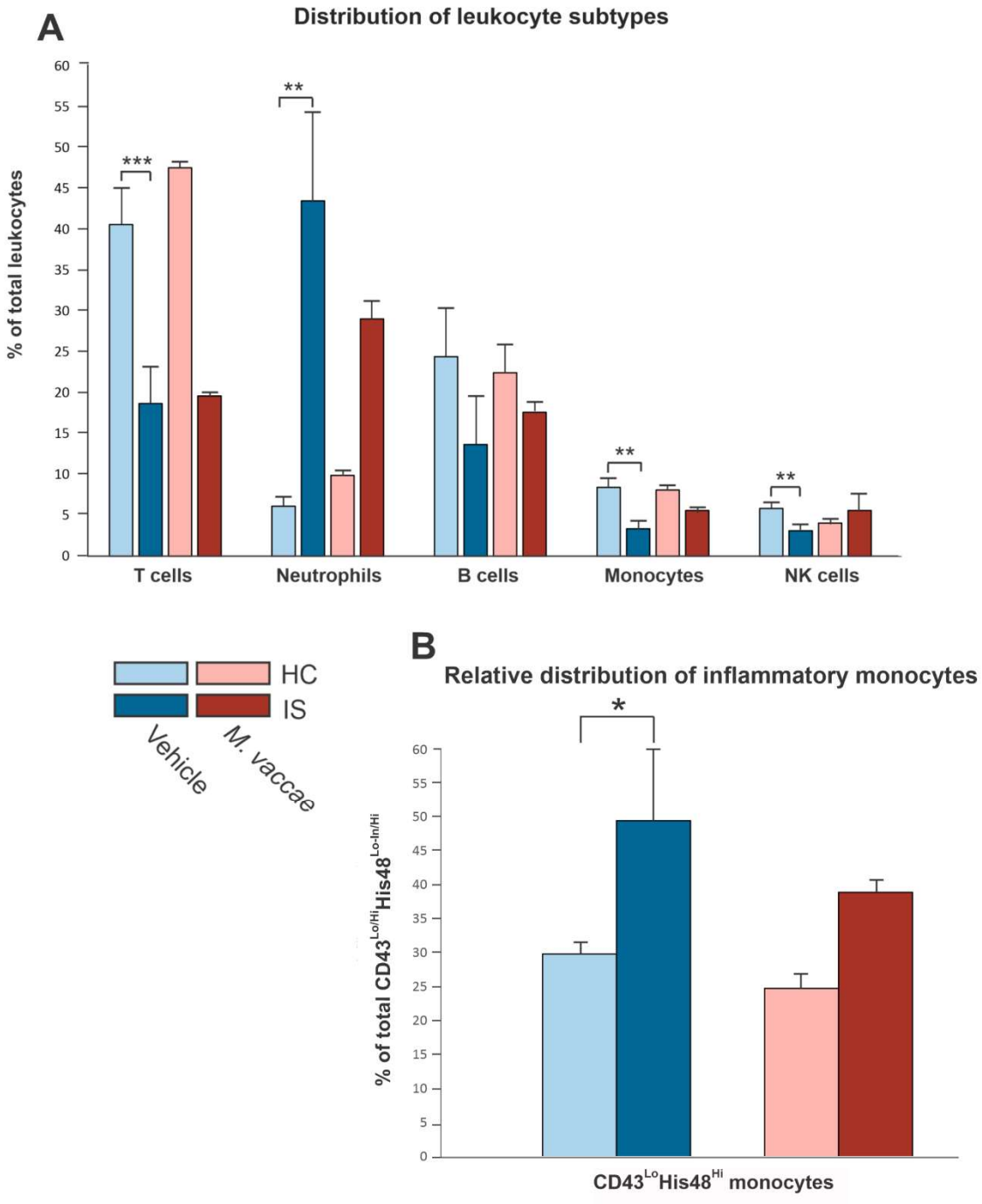

Fig. 6. Inescapable tail shock stress (IS) alters the distribution of leukocyte subpopulations in peripheral blood six hours after IS termination. Data represent (**A**) the distribution of leukocyte subtypes and (**B**) the relative distribution of inflammatory monocytes in BBS/HC, $n = 4$; BBS/IS, $n = 4$; *M. vaccae*/HC, $n = 2$; *M. vaccae*/IS, $n = 2$. Bars represent mean + SD. $*p < 0.05$, $**p < 0.01$, $***p < 0.001$.

3.2. Effect of IS on the relative distribution of inflammatory monocytes.

IS induced changes in the relative abundance of $CD43^{Lo}His48^{Hi}$ inflammatory monocytes relative to all monocytes (**Fig. 6.B)**. IS significantly increased the relative abundance of $CD43^{Lo}His48^{Hi}$ monocytes in the peripheral blood of BBS/IS rats compared to BBS/HC rats [$t(6) = 6.79$, $p < 0.05$]. *M. vaccae*/IS animals qualitatively showed an increase of inflammatory monocytes compared to *M. vaccae*/HC animals.

4. Discussion

Given that peripheral blood was sampled six hours after IS termination, rats exposed to IS in both BBS and *M. vaccae* NCTC 11659 groups displayed a change in the distribution of leukocyte subpopulations that is consistent with a previous study examining stress-induced mobilization of immune cells (Dhabhar et al., 2012), which showed an increase in neutrophils mirrored by decreases in lymphocytes 120 minutes after acute stress. Our results show that the change in leukocyte distribution persists even six hours after the termination of a stressor. Similar to the RSD model, which shows an increase in the percentage of inflammatory monocytes in the blood 0.5 days after the last cycle of social defeat in mice (Wohleb, McKim, Shea, et al., 2014), the percentage of inflammatory monocytes was significantly increased 6 hours after IS, suggesting that IS may be robust enough to elicit similar effects as seen in RSD models; however, this cannot be confirmed since blood samples were not taken at the same various timepoints in the RSD model.

Although the results of *M. vaccae* NCTC 11659-treated groups cannot be statistically quantified due to insufficient samples in the *M. vaccae* NCTC 11659-treated groups ($n = 2$), *M. vaccae* NCTC 11659 seemed to prevent the increase of the relative abundance of inflammatory monocytes in the peripheral blood. Adding more animals to treatment groups will allow for further and definitive analysis to elucidate the effects of *M. vaccae* NCTC 11659 on inflammatory monocytes and other leukocyte subpopulations. If *M. vaccae* NCTC 11659 does indeed prevent the increase of inflammatory monocytes, this would support the hypothesis that *M. vaccae* NCTC 11659 achieves its stress-resilience effects by mitigating the proinflammatory signaling of inflammatory monocytes by inhibiting the differentiation of inflammatory monocytes or by preventing the release of these

monocytes into circulation from the bone marrow. However, the mechanisms through which this would be achieved is not known and may be independent on any effects that *M. vaccae* NCTC 11659 may have on the hypothalamic-pituitary-adrenal (HPA) axis since *M. vaccae* NCTC 11659 has no effect on HPA axis responses to psychosocial stress (Reber et al., 2016).

Another potential mechanism through which *M. vaccae* NCTC 11659 exerts its effects may be due to interactions between monocytes and other lymphocytes, such as CD4+ T cells. The decrease in leukocyte numbers in the peripheral blood does not necessarily mean that there is a decrease of immune system activation. Rather, a decrease in lymphocyte numbers in the periphery is an indication that immune cells are being trafficked out of circulation into the "battle grounds", specific organs or tissues that are targeted during stress (Dhabhar et al., 2012). Inflammatory monocytes that secrete proinflammatory cytokines such interleukin 1 beta protein (IL-1β), interleukin 23 (IL-23), and interleukin 6 (IL-6), are capable of driving CD4 cells into an inflammatory Th17 phenotype, which has been shown to increase the severity of chronic inflammatory conditions such as rheumatoid arthritis (Roberts et al., 2015).

In order to gain a better understanding of *M. vaccae* NCTC 11659's role in immunoregulation, future studies should look at analyzing leukocyte subpopulations at different time points. One timepoint of interest would be to collect leukocyte samples before and after injection with *M. vaccae* NCTC 11659. Understanding any changes in leukocyte subpopulations after *M. vaccae* NCTC 11659 treatment would provide a better clue of how *M. vaccae* NCTC 11659 initially starts exerting its immunoregulatory effects. Additionally, analyzing leukocyte subpopulations in other models of stress where *M. vaccae* NCTC 11659 has been shown to have stress-resilience effects, such as fear-potentiated startle, may provide clues into whether *M. vaccae* NCTC 11659 achieves those effects through similar mechanisms shown during JSE after IS exposure. Since the feasibility of running a nine color flow cytometry panel was confirmed in this experiment, a modified nine color panel can be created using different cell markers allowing further investigation into different leukocyte subtypes. For example, infiltrating monocytes are characterized by increased c-c chemokine receptor type 2 (CCR2) expression (Miller & Raison, 2016). CCR2 antibody can then be used to identify infiltrating monocytes

and may be used in conjunction with another analysis identifying brain regions that highly express c-c chemokine ligand type 2 (CCL2), which may help map more precisely which areas of the brain are being targeting by these inflammatory monocytes.

References

Amoroso, M., Bottcher, A., Lowry, C. A., Langgartner, D., & Reber, S. O. (2020). Subcutaneous Mycobacterium vaccae promotes resilience in a mouse model of chronic psychosocial stress when administered prior to or during psychosocial stress. *Brain Behav Immun*, *87*, 309-317. https://doi.org/10.1016/j.bbi.2019.12.018

Barnett-Vanes, A., Sharrock, A., Birrell, M. A., & Rankin, S. (2016). A Single 9-Colour Flow Cytometric Method to Characterise Major Leukocyte Populations in the Rat: Validation in a Model of LPS-Induced Pulmonary Inflammation. *PLoS One*, *11*(1), e0142520. https://doi.org/10.1371/journal.pone.0142520

Bowers, S. J., Lambert, S., He, S., Lowry, C. A., Fleshner, M., Wright, K. P., Jr., Turek, F. W., & Vitaterna, M. H. (2020). Immunization with a heat-killed bacterium, Mycobacterium vaccae NCTC 11659, prevents the development of cortical hyperarousal and a PTSD-like sleep phenotype after sleep disruption and acute stress in mice. *Sleep*. https://doi.org/10.1093/sleep/zsaa271

Dantzer, R., O'Connor, J. C., Freund, G. G., Johnson, R. W., & Kelley, K. W. (2008). From inflammation to sickness and depression: when the immune system subjugates the brain. *Nat Rev Neurosci*, *9*(1), 46-56. https://doi.org/10.1038/nrn2297

Davis, M. T., Holmes, S. E., Pietrzak, R. H., & Esterlis, I. (2017). Neurobiology of Chronic Stress-Related Psychiatric Disorders: Evidence from Molecular Imaging Studies. *Chronic Stress (Thousand Oaks)*, *1*. https://doi.org/10.1177/2470547017710916

Dhabhar, F. S., Malarkey, W. B., Neri, E., & McEwen, B. S. (2012). Stress-induced redistribution of immune cells—From barracks to boulevards to battlefields: A tale of three hormones – Curt Richter Award Winner. *Psychoneuroendocrinology*, *37*(9), 1345-1368. https://doi.org/10.1016/j.psyneuen.2012.05.008

Dhabhar, F. S., Miller, A. H., Stein, M., McEwen, B. S., & Spencer, R. L. (1994). Diurnal and acute stress-induced changes in distribution of peripheral blood leukocyte subpopulations. *Brain Behav Immun*, *8*(1), 66-79. https://doi.org/10.1006/brbi.1994.1006

Foertsch, S., Füchsl, A. M., Faller, S. D., Hölzer, H., Langgartner, D., Messmann, J., Strauß, G., & Reber, S. O. (2017). Splenic glucocorticoid resistance following psychosocial stress requires physical injury. *Scientific reports*, *7*(1), 15730-15730. https://doi.org/10.1038/s41598-017-15897-2

Fonken, L. K., Frank, M. G., D'Angelo, H. M., Heinze, J. D., Watkins, L. R., Lowry, C. A., & Maier, S. F. (2018). Mycobacterium vaccae immunization protects aged rats from surgery-elicited neuroinflammation and cognitive dysfunction. *Neurobiol Aging*, *71*, 105-114. https://doi.org/10.1016/j.neurobiolaging.2018.07.012

Fox, J. H., Hassell, J. E., Jr., Siebler, P. H., Arnold, M. R., Lamb, A. K., Smith, D. G., Day, H. E. W., Smith, T. M., Simmerman, E. M., Outzen, A. A., Holmes, K. S., Brazell, C. J., & Lowry, C. A. (2017).

Preimmunization with a heat-killed preparation of Mycobacterium vaccae enhances fear extinction in the fear-potentiated startle paradigm. *Brain Behav Immun*, *66*, 70-84. https://doi.org/10.1016/j.bbi.2017.08.014

Foxx, C. L., Heinze, J. D., Gonzalez, A., Vargas, F., Baratta, M. V., Elsayed, A. I., Stewart, J. R., Loupy, K. M., Arnold, M. R., Flux, M. C., Sago, S. A., Siebler, P. H., Milton, L. N., Lieb, M. W., Hassell, J. E., Smith, D. G., Lee, K. A. K., Appiah, S. A., Schaefer, E. J., Panitchpakdi, M., Sikora, N. C., Weldon, K. C., Stamper, C. E., Schmidt, D., Duggan, D. A., Mengesha, Y. M., Ogbaselassie, M., Nguyen, K. T., Gates, C. A., Schnabel, K., Tran, L., Jones, J. D., Vitaterna, M. H., Turek, F. W., Fleshner, M., Dorrestein, P. C., Knight, R., Wright, K. P., & Lowry, C. A. (2020). Effects of Immunization With the Soil-Derived Bacterium Mycobacterium vaccae on Stress Coping Behaviors and Cognitive Performance in a "Two Hit" Stressor Model. *Front Physiol*, *11*, 524833. https://doi.org/10.3389/fphys.2020.524833

Frank, M. G., Fonken, L. K., Dolzani, S. D., Annis, J. L., Siebler, P. H., Schmidt, D., Watkins, L. R., Maier, S. F., & Lowry, C. A. (2018). Immunization with Mycobacterium vaccae induces an anti-inflammatory milieu in the CNS: Attenuation of stress-induced microglial priming, alarmins and anxiety-like behavior. *Brain Behav Immun*, *73*, 352-363. https://doi.org/10.1016/j.bbi.2018.05.020

Hassell, J. E., Jr., Fox, J. H., Arnold, M. R., Siebler, P. H., Lieb, M. W., Schmidt, D., Spratt, E. J., Smith, T. M., Nguyen, K. T., Gates, C. A., Holmes, K. S., Schnabel, K. S., Loupy, K. M., Erber, M., & Lowry, C. A. (2019). Treatment with a heat-killed preparation of Mycobacterium vaccae after fear conditioning enhances fear extinction in the fear-potentiated startle paradigm. *Brain Behav Immun*, *81*, 151-160. https://doi.org/10.1016/j.bbi.2019.06.008

Hasselmann, H., Gamradt, S., Taenzer, A., Nowacki, J., Zain, R., Patas, K., Ramien, C., Paul, F., Wingenfeld, K., Piber, D., Gold, S. M., & Otte, C. (2018). Pro-inflammatory Monocyte Phenotype and Cell-Specific Steroid Signaling Alterations in Unmedicated Patients With Major Depressive Disorder. *Front Immunol*, *9*, 2693. https://doi.org/10.3389/fimmu.2018.02693

Judd, L. L., Paulus, M. P., Wells, K. B., & Rapaport, M. H. (1996). Socioeconomic burden of subsyndromal depressive symptoms and major depression in a sample of the general population. *Am J Psychiatry*, *153*(11), 1411-1417. https://doi.org/10.1176/ajp.153.11.1411

Kelly, J. R., Minuto, C., Cryan, J. F., Clarke, G., & Dinan, T. G. (2017). Cross Talk: The Microbiota and Neurodevelopmental Disorders. *Front Neurosci*, *11*, 490. https://doi.org/10.3389/fnins.2017.00490

Kessler, R., & Greenberg, P. (2002). The economic burden of anxiety and stress disorders. *Neuropsychopharmacology: The Fifth Generation of Progress*, *67*, 981-992.

Kessler, R. C. (2000). Posttraumatic stress disorder: the burden to the individual and to society. *J Clin Psychiatry*, *61 Suppl 5*, 4-12; discussion 13-14. https://www.ncbi.nlm.nih.gov/pubmed/10761674

Kipnis, J. (2018). Immune system: The "seventh sense". *J Exp Med*, *215*(2), 397-398. https://doi.org/10.1084/jem.20172295

Loupy, K. M., Arnold, M. R., Hassell, J. E., Jr., Lieb, M. W., Milton, L. N., Cler, K. E., Fox, J. H., Siebler, P. H., Schmidt, D., Noronha, S., Day, H. E. W., & Lowry, C. A. (2019). Evidence that preimmunization with a heat-killed preparation of Mycobacterium vaccae reduces corticotropin-releasing hormone mRNA expression in the extended amygdala in a fear-potentiated startle paradigm. *Brain Behav Immun*, *77*, 127-140. https://doi.org/10.1016/j.bbi.2018.12.015

Loupy, K. M., Cler, K. E., Marquart, B. M., Yifru, T. W., D'Angelo, H. M., Arnold, M. R., Elsayed, A. I., Gebert, M. J., Fierer, N., Fonken, L. K., Frank, M. G., Zambrano, C. A., Maier, S. F., & Lowry, C. A. (2021). Comparing the effects of two different strains of mycobacteria, Mycobacterium vaccae NCTC 11659 and M. vaccae ATCC 15483, on stress-resilient behaviors and lipid-immune signaling in rats. *Brain Behav Immun*, *91*, 212-229. https://doi.org/10.1016/j.bbi.2020.09.030

Lowry, C. A., Hollis, J. H., de Vries, A., Pan, B., Brunet, L. R., Hunt, J. R. F., Paton, J. F. R., van Kampen, E., Knight, D. M., Evans, A. K., Rook, G. A. W., & Lightman, S. L. (2007). Identification of an immune-responsive mesolimbocortical serotonergic system: Potential role in regulation of emotional behavior. *Neuroscience*, *146*(2), 756-772. https://doi.org/https://doi.org/10.1016/j.neuroscience.2007.01.067

Lowry, C. A., Smith, D. G., Siebler, P. H., Schmidt, D., Stamper, C. E., Hassell, J. E., Jr., Yamashita, P. S., Fox, J. H., Reber, S. O., Brenner, L. A., Hoisington, A. J., Postolache, T. T., Kinney, K. A., Marciani, D., Hernandez, M., Hemmings, S. M., Malan-Muller, S., Wright, K. P., Knight, R., Raison, C. L., & Rook, G. A. (2016). The Microbiota, Immunoregulation, and Mental Health: Implications for Public Health. *Curr Environ Health Rep*, *3*(3), 270-286. https://doi.org/10.1007/s40572-016-0100-5

Maslanik, T., Tannura, K., Mahaffey, L., Loughridge, A. B., Benninson, L., Ursell, L., Greenwood, B. N., Knight, R., & Fleshner, M. (2012). Commensal Bacteria and MAMPs Are Necessary for Stress-Induced Increases in IL-1β and IL-18 but Not IL-6, IL-10 or MCP-1. *PLoS One*, *7*(12), e50636. https://doi.org/10.1371/journal.pone.0050636

Miller, A. H., & Raison, C. L. (2016). The role of inflammation in depression: from evolutionary imperative to modern treatment target. *Nat Rev Immunol*, *16*(1), 22-34. https://doi.org/10.1038/nri.2015.5

Miller, G. E., Chen, E., Sze, J., Marin, T., Arevalo, J. M. G., Doll, R., Ma, R., & Cole, S. W. (2008). A functional genomic fingerprint of chronic stress in humans: blunted glucocorticoid and increased NF-kappaB signaling. *Biological Psychiatry*, *64*(4), 266-272. https://doi.org/10.1016/j.biopsych.2008.03.017

O'Brien, M. E. R., Anderson, H., Kaukel, E., O'Byrne, K., Pawlicki, M., Von Pawel, J., & Reck, M. (2004). SRL172 (killed Mycobacterium vaccae) in addition to standard chemotherapy improves quality of life

without affecting survival, in patients with advanced non-small-cell lung cancer: phase III results. *Annals of Oncology*, *15*(6), 906-914. https://doi.org/10.1093/annonc/mdh220

Percie du Sert, N., Hurst, V., Ahluwalia, A., Alam, S., Avey, M. T., Baker, M., Browne, W. J., Clark, A., Cuthill, I. C., Dirnagl, U., Emerson, M., Garner, P., Holgate, S. T., Howells, D. W., Karp, N. A., Lazic, S. E., Lidster, K., MacCallum, C. J., Macleod, M., Pearl, E. J., Petersen, O. H., Rawle, F., Reynolds, P., Rooney, K., Sena, E. S., Silberberg, S. D., Steckler, T., & Wurbel, H. (2020). The ARRIVE guidelines 2.0: Updated guidelines for reporting animal research. *PLoS Biol*, *18*(7), e3000410. https://doi.org/10.1371/journal.pbio.3000410

Powell, N. D., Sloan, E. K., Bailey, M. T., Arevalo, J. M., Miller, G. E., Chen, E., Kobor, M. S., Reader, B. F., Sheridan, J. F., & Cole, S. W. (2013). Social stress up-regulates inflammatory gene expression in the leukocyte transcriptome via beta-adrenergic induction of myelopoiesis. *Proc Natl Acad Sci U S A*, *110*(41), 16574-16579. https://doi.org/10.1073/pnas.1310655110

Reader, B. F., Jarrett, B. L., McKim, D. B., Wohleb, E. S., Godbout, J. P., & Sheridan, J. F. (2015). Peripheral and central effects of repeated social defeat stress: monocyte trafficking, microglial activation, and anxiety. *Neuroscience*, *289*, 429-442. https://doi.org/10.1016/j.neuroscience.2015.01.001

Reber, S. O., Siebler, P. H., Donner, N. C., Morton, J. T., Smith, D. G., Kopelman, J. M., Lowe, K. R., Wheeler, K. J., Fox, J. H., Hassell, J. E., Jr., Greenwood, B. N., Jansch, C., Lechner, A., Schmidt, D., Uschold-Schmidt, N., Fuchsl, A. M., Langgartner, D., Walker, F. R., Hale, M. W., Lopez Perez, G., Van Treuren, W., Gonzalez, A., Halweg-Edwards, A. L., Fleshner, M., Raison, C. L., Rook, G. A., Peddada, S. D., Knight, R., & Lowry, C. A. (2016). Immunization with a heat-killed preparation of the environmental bacterium Mycobacterium vaccae promotes stress resilience in mice. *Proc Natl Acad Sci U S A*, *113*(22), E3130-3139. https://doi.org/10.1073/pnas.1600324113

Roberts, C. A., Dickinson, A. K., & Taams, L. S. (2015). The Interplay Between Monocytes/Macrophages and CD4(+) T Cell Subsets in Rheumatoid Arthritis. *Front Immunol*, *6*, 571. https://doi.org/10.3389/fimmu.2015.00571

Rook, G. A., Adams, V., Hunt, J., Palmer, R., Martinelli, R., & Brunet, L. R. (2004). Mycobacteria and other environmental organisms as immunomodulators for immunoregulatory disorders. *Springer Semin Immunopathol*, *25*(3-4), 237-255. https://doi.org/10.1007/s00281-003-0148-9

Rook, G. A., Raison, C. L., & Lowry, C. A. (2014). Microbial 'old friends', immunoregulation and socioeconomic status. *Clin Exp Immunol*, *177*(1), 1-12. https://doi.org/10.1111/cei.12269

Weber, M. D., Godbout, J. P., & Sheridan, J. F. (2017). Repeated Social Defeat, Neuroinflammation, and Behavior: Monocytes Carry the Signal. *Neuropsychopharmacology*, *42*(1), 46-61. https://doi.org/10.1038/npp.2016.102

Wohleb, E. S., McKim, D. B., Shea, D. T., Powell, N. D., Tarr, A. J., Sheridan, J. F., & Godbout, J. P. (2014). Re-establishment of anxiety in stress-sensitized mice is caused by monocyte trafficking from the spleen to the brain. *Biol Psychiatry*, *75*(12), 970-981. https://doi.org/10.1016/j.biopsych.2013.11.029

Wohleb, E. S., McKim, D. B., Sheridan, J. F., & Godbout, J. P. (2014). Monocyte trafficking to the brain with stress and inflammation: a novel axis of immune-to-brain communication that influences mood and behavior. *Front Neurosci*, *8*, 447. https://doi.org/10.3389/fnins.2014.00447

Xu, M., Wang, C., Krolick, K. N., Shi, H., & Zhu, J. (2020). Difference in post-stress recovery of the gut microbiome and its altered metabolism after chronic adolescent stress in rats. *Sci Rep*, *10*(1), 3950. https://doi.org/10.1038/s41598-020-60862-1

Yang, J., Zhang, L., Yu, C., Yang, X.-F., & Wang, H. (2014). Monocyte and macrophage differentiation: circulation inflammatory monocyte as biomarker for inflammatory diseases. *Biomarker research*, *2*(1), 1-1. https://doi.org/10.1186/2050-7771-2-1

Zuany-Amorim, C., Sawicka, E., Manlius, C., Le Moine, A., Brunet, L. R., Kemeny, D. M., Bowen, G., Rook, G., & Walker, C. (2002). Suppression of airway eosinophilia by killed Mycobacterium vaccae-induced allergen-specific regulatory T-cells. *Nature Medicine*, *8*(6), 625-629. https://doi.org/10.1038/nm0602-625